Earth and Planetary Science Letters 270 (2008) 106–118

Contents lists available at ScienceDirect

Earth and Planetary Science Letters

journal homepage: www.elsevier.com/locate/epsl

Hf–W thermochronometry: Closure temperature and constraints on the accretion and cooling history of the H chondrite parent body

Thorsten Kleine [a,*], Mathieu Touboul [a], James A. Van Orman [b], Bernard Bourdon [a], Colin Maden [a], Klaus Mezger [c], Alex N. Halliday [d]

[a] Institute for Isotope Geochemistry and Mineral Resources, Department of Earth Sciences, ETH Zurich, Clausiusstrasse 25, 8092 Zurich, Switzerland
[b] Department of Geological Sciences, Case Western Reserve University, 10900 Euclid Ave, Cleveland, Ohio 44106-7216, United States
[c] Institut für Mineralogie, Universität Münster, Corrensstrasse 24, 48149 Münster, Germany
[d] Department of Earth Sciences, University of Oxford, Parks Road, OX1 3PR, United Kingdom

ARTICLE INFO

Article history:
Received 19 December 2007
Received in revised form 3 March 2008
Accepted 4 March 2008
Available online 15 March 2008

Editor: R.W. Carlson

Keywords:
W isotopes
closure temperature
H chondrites
thermochronometry
chondrules

ABSTRACT

We obtained Hf–W metal-silicate isochrons for several H chondrites of petrologic types 4, 5, and 6 to constrain the accretion and high-temperature thermal history of the H chondrite parent body. The silicate fractions have $^{180}Hf/^{184}W$ ratios up to ~51 and $^{182}W/^{184}W$ ratios up to ~33 ε units higher than the whole-rock. These high $^{180}Hf/^{184}W$ and radiogenic W isotope ratios result in highly precise Hf–W ages. The Hf–W ages of the H chondrites become younger with increasing metamorphic grade and range from $\Delta t_{CAI} = 1.7 \pm 0.7$ Ma for the H4 chondrite Ste. Marguerite to $\Delta t_{CAI} = 9.6 \pm 1.0$ Ma for the H6 chondrites Kernouvé and Estacado. Closure temperatures for the Hf–W system in H chondrites were estimated from numerical simulations of W diffusion in high-Ca pyroxene, the major host of radiogenic ^{182}W in H chondrites, and range from 800±50 °C for H4 chondrites to 875±75 °C for H6 chondrites. Owing to these high closure temperatures, the Hf–W system closed early and dates processes associated with the earliest evolution of the H chondrite parent body. Consequently, the high-temperature interval of ~8 Ma as defined by the Hf–W ages is much shorter than intervals obtained from Rb–Sr and Pb–Pb dating. For H4 chondrites, heating on the parent body probably was insufficient to cause W diffusion in high-Ca pyroxene, such that the Hf–W age of $\Delta t_{CAI} = 1.7 \pm 0.7$ Ma for Ste. Marguerite was not reset and most likely dates chondrule formation. This is consistent with Al–Mg ages of ~2 Ma for L and LL chondrules and indicates that chondrules from all ordinary chondrites formed contemporaneously. The Hf–W ages for H5 and H6 chondrites of $\Delta t_{CAI} = 5.9 \pm 0.9$ Ma and $\Delta t_{CAI} = 9.6 \pm 1.0$ Ma correspond closely to the time of the thermal peak within the H chondrite parent body. Combined with previously published chronological data the Hf–W ages reveal an inverse correlation of cooling rate and metamorphic grade: shortly after their thermal peak H6 chondrites cooled at ~10 °C/Ma, H5 chondrites at ~30 °C/Ma and H4 chondrites at ~55 °C/Ma. These Hf–W age constraints are most consistent with an onion-shell structure of the H chondrite parent body that was heated internally by energy released from ^{26}Al decay. Parent body accretion started after chondrule formation at 1.7±0.7 Ma and probably ended before 5.9±0.9 Ma, when parts of the H chondrite parent body already had cooled from their thermal peak. The well-preserved cooling curves for the H chondrites studied here indicate that these samples derive from a part of the H chondrite parent body that remained largely unaffected by impact disruption and reassembly but such processes might have been important in other areas. The H chondrite parent body has a $^{180}Hf/^{184}W$ ratio of 0.63±0.20, distinctly lower than the $^{180}Hf/^{184}W = 1.21 \pm 0.06$ of carbonaceous chondrite parent bodies. This difference reflects Hf–W fractionation within the first ~2 Ma of the solar system, presumably related to processes in the solar nebula.

1. Introduction

Hafnium–tungsten chronometry has been applied widely to determine the timescales of differentiation of asteroids and terrestrial planets (Harper and Jacobsen, 1996; Schoenberg et al., 2002; Yin et al., 2002; Halliday, 2004; Kleine et al., 2004b; Jacobsen, 2005; Nimmo and Agnor, 2006; Nimmo and Kleine, 2007) but its potential for dating chondrites and constraining the thermal evolution of their parent bodies has yet to be explored. To utilize Hf–W chronometry of meteorites meaningfully it is necessary to know the closure temperature (T_c) for diffusive exchange of parent and daughter elements among the different minerals in a rock (Dodson, 1973; Ganguly and

* Corresponding author.
E-mail address: kleine@erdw.ethz.ch (T. Kleine).

0012-821X © 2008 Elsevier B.V. Open access under CC BY-NC-ND license.
doi:10.1016/j.epsl.2008.03.013

Tirone, 2001). Knowledge of T_c is essential for evaluating whether an age dates the time of mineral growth or some time along the cooling path. Such information is critical for the interpretation of Hf–W ages in comparison to results from other chronometers and within the framework of models for the thermal evolution of asteroids.

Closure temperatures can be calculated from diffusion rates of the element of interest in the appropriate minerals. Such data are not available for W but here we determine closure temperatures from numerical simulations of W diffusion in silicates using the model of Van Orman et al. (2001, 2006). These results are compared to values of T_c estimated by age comparison. Ideal samples for this (i) should be well dated with different chronometers (i.e., have a well-defined cooling history), (ii) should exhibit protracted cooling, such that differences in closure temperatures result in well-resolved age differences, and (iii) should contain components having substantially different Hf/W ratios, such that precise Hf–W isochrons can be determined. These criteria are met by ordinary chondrites. First, the thermal evolution and structure of their parent bodies has already been studied with several chronometers (Wasserburg et al., 1969; Podosek and Brannon, 1991; Göpel et al., 1994; Trieloff et al., 2003; Amelin et al., 2005; Bouvier et al., 2007). Second, ordinary chondrites exhibit a wide range of metamorphic conditions from type 3 (unequilibrated) to type 6 (highly equilibrated), reflecting widely different cooling histories (Dodd, 1969). Third, ordinary chondrites contain abundant metal, which makes them ideal for Hf–W chronometry. Metals are virtually Hf–free but are enriched in W, resulting in $^{180}Hf/^{184}W \sim 0$ in metals and elevated $^{180}Hf/^{184}W$ ratios in the corresponding silicates. For instance, Kleine et al. (2002) reported $^{180}Hf/^{184}W \sim 14$ coupled with radiogenic $^{182}W/^{184}W$ for a silicate fraction from the H4 chondrite Ste. Marguerite. Such high $^{180}Hf/^{184}W$ and radiogenic $^{182}W/^{184}W$ ratios make it possible to obtain high-precision Hf–W ages.

We present Hf–W isochrons for several equilibrated H chondrites. Most of the samples investigated here were previously dated with other chronometers, including the ^{207}Pb–^{206}Pb system (Göpel et al., 1994; Amelin et al., 2005; Bouvier et al., 2007). The diffusivity of Pb in the relevant minerals is relatively well constrained (Cherniak et al., 1991; Cherniak, 1998), facilitating estimates of closure temperatures by age comparison. These estimates are compared to results from numerical simulations of W diffusion in a metal-silicate assemblage, which, in conjunction with the Hf–W ages, are used to assess the significance of the Hf–W ages and to constrain the thermal evolution of the H chondrite parent asteroid.

2. Analytical methods

Pieces of meteorite were cleaned with abrasive paper and with 0.05 M HNO_3, de-ionized H_2O and ethanol in an ultrasonic bath to remove any contamination introduced during cutting from larger samples. Each fragment was crushed in an agate mortar and separated into <40 μm and 40–150 μm fractions using nylon sieves. During crushing metal grains were removed using a hand-magnet and separated into two fractions using a 40 μm nylon sieve.

Where sufficient material was available, the coarser fraction was further separated into several fractions, depending on the size of the metal grains. Silicate dust attached to or intergrown with the metal grains was removed by repeated crushing of the magnetic fraction under ethanol. Although all visible metal grains were removed, the 40–150 μm fractions were still slightly magnetic, most likely reflecting the presence of tiny metal inclusions in the silicate and oxide grains. The 40–150 μm fractions were further separated using a hand-magnet to obtain several "non-magnetic" fractions. These were labeled NM-n, $n = 1, 2, 3\ldots$, NM-1 always denoting the least magnetic fraction for each chondrite. The NM-1 fractions are non- magnetic (i.e., with the hand-magnet used here) and might be entirely metal-free, the NM-2 fractions are slightly more magnetic, and the NM-3 fractions again are slightly more magnetic than the NM-2 fractions.

All NM fractions were inspected under the binocular microscope. They consist mainly of olivine and pyroxene but most fractions also contain some ilmenite, feldspar and phosphates. All NM fractions were cleaned with ethanol in an ultrasonic bath and powdered in an agate mortar. Remaining metal grains were removed from these powders using a hand-magnet.

The metal separates were dissolved in 15 mL Savillex® vials at ~120 °C on a hotplate using 6 M HCl–0.06 M HF. In some cases, a few drops of concentrated HNO_3 were added. The NM fractions were dissolved in 60 mL Savillex® vials at ~180 °C on a hotplate using HF–HNO_3–$HClO_4$ (5:4:1). After digestion, the samples were dried and re-dissolved in HNO_3–H_2O_2 to remove organic compounds. Then the samples were completely dissolved in 6 M HCl–0.06 M HF and a ~10% aliquot was spiked with a mixed ^{180}Hf–^{183}W tracer that was calibrated against pure Hf and W metals (Kleine et al., 2004a).

The methods for the separation of Hf and W from the sample matrix were slightly modified from those outlined in Kleine et al. (2004a). The metal separates were dried, re-dissolved in 1 M HF–0.1 M HNO_3 and loaded onto pre-cleaned anion exchange columns (2 mL BioRad® AG1X8, 200–400 mesh). The matrix was washed from the column using ~5 resin volumes 1 M HF–0.1 M HNO_3 and W together with other high field strength elements and Mo was eluted in 6 M HNO_3–0.2 M HF (Münker et al., 2001; Weyer et al., 2002; Kleine et al., 2004a). After drying down, the W cut was re-dissolved in 1 M HF–0.1 M HNO_3 and loaded onto a pre-cleaned anion exchange column (1 mL BioRad® AG1X8, 200–400 mesh).

Again, the matrix was washed from the column using ~5 resin volumes 1 M HF–0.1 M HNO_3 but high field strength elements (Hf, Zr, Nb, Ti) were first removed in 6 M HCl–0.01 M HF before W was eluted in 6 M HCl–1 M HF. In this acid mixture, Mo is strongly adsorbed on the anion resin (Kleine et al., 2004a).

The first part of the ion exchange procedure employed for the NM fractions is similar to the first step in the Hf chemistry of Salters and Hart (Salters and Hart, 1991). After aliquoting, the NM fractions were dried and re-dissolved in 4 M HF. The solution was centrifuged and decanted and the residue washed several times with 4 M HF. The solution was ultrasonicated several times to ensure optimal release of W from the fluoride residue and was loaded onto pre-cleaned anion exchange columns (3.5 mL BioRad® AG1X8, 100–200 mesh). The matrix was washed from the column using ~6 resin volumes of 4 M HF and W together with Zr, Hf, Ti, Nb, Mo was eluted using 6 M HNO_3–0.2 M HF. After drying, this cut was re-dissolved in 1 M HCl–0.5 M HF and loaded onto pre-cleaned anion exchange columns (3 mL BioRad® AG1X8, 100–200 mesh), where W was purified following the procedure of Kleine et al. (2004a). Titanium was washed from the column using HAc–HNO_3–H_2O_2, Zr, Hf, and Nb were rinsed off in 6 M HCl–0.01 M HF and W was eluted in 6 M HCl–1 M HF.

Total procedural blanks ranged from ~50 to ~350 pg for the W isotope composition measurements and ~12 to 50 pg W and ~10 pg Hf for the isotope dilution measurements. The variable W blanks are caused by the use of different batches of acetic acid.

All isotope measurements were performed using a *Nu Plasma* MC-ICP-MS at ETH Zürich, equipped with a Cetac Aridus desolvating nebuliser. Prior to measurement, the samples were re-dissolved and dried several times in HNO_3–H_2O_2 to remove organic compounds and, in the case of metal-rich samples, volatile Os oxides and then taken up in a 0.56 M HNO_3–0.24 M HF mixture. Tungsten isotope compositions of metals and whole-rocks were typically measured with a signal intensity of ~2 V on ^{182}W, which was obtained for a ~20 ppb W solution. For these samples, 60 ratios (3 blocks of 20 ratios) were measured resulting in within-run statistics of the order of 0.2 ε units (2σ). Owing to the low W contents in the NM fractions, their W isotope compositions were measured in 1 or 2 blocks of 20 ratios each with signal intensities of ~0.5 to 1 V on ^{182}W. The within-run statistics of these measurements were typically between 0.5 and 1 ε unit. Instrumental mass bias was corrected relative to $^{186}W/^{183}W = 1.9859$

using the exponential law. Small isobaric interferences of Os on masses 184 and 186 were corrected by monitoring ^{188}Os and were negligible. The ^{182}W/^{184}W and ^{183}W/^{184}W ratios of all samples were determined relative to two standard runs bracketing the sample run and are reported in ε^{18i}W units, which is the deviation of the ^{18i}W/^{184}W ratio from the terrestrial standard value in parts per 10,000. The reproducibility of the ~20 ppb standard during one measurement day is typically equal to or better than ~0.3 ε units (2 SD) for the ^{182}W/^{184}W ratio and ~0.2 ε units (2 SD) for the ^{183}W/^{184}W ratio. The external reproducibility of the W isotope measurements typically is 0.3–0.4 ε units (2 SD) for the ^{182}W/^{184}W ratio and 0.2–0.3 ε units (2 SD) for the ^{183}W/^{184}W ratio and was estimated by repeated analysis of a whole-rock powder of the Kernouvé H6 chondrite and several H chondrite metals (Table 1). The external reproducibility of the isotope measurements of these samples is similar to those obtained for the W standard during one measurement session, indicating that matrix effects are minor to absent. The uncertainties for the W isotope measurements of the W-poor NM fractions (i.e., most of the NM-1 and -2 fractions) were assessed by repeated measurement (1 block of 20 ratios each) of a ~10 ppb W standard solutions that yielded an external reproducibility of

Table 1
Hf–W data for metals, whole-rocks and non-magnetic fractions

Sample	Hf (ppb)	W (ppb)	^{180}Hf/^{184}W	ε^{182}W±2σ meas.	ε^{182}W±2σ corr.	ε^{183}W±2σ
Ste. Marguerite (H4)						
Metal	1.81	823.0	0.00251±2	−3.20±0.25		0.05±0.15
				−3.19±0.18		−0.21±0.12
				−3.13±0.19		0.02±0.14
Mean				−3.18±0.07		−0.05±0.29
NM	223.0	16.31	15.6±1	12.8±0.3		2.9±0.2
Richardton (H5)						
A-metal (>150 μm)	30.34	660.9	0.0523±4	−3.47±0.19		−0.05±0.11
				−3.32±0.19		0.06±0.13
				−3.27±0.20		−0.03±0.12
				−3.06±0.18		0.17±0.16
Mean				−3.28±0.35		0.04±0.20
A-NM-1	212.9	18.31	13.3±2	6.9±0.4	7.4±0.8	0.03±0.19
Repl.	212.1	18.23	13.3±1	5.9±0.5	6.9±1.4	0.97±0.52
A-NM-2	174.9	18.28	10.9±3	4.1±0.5	4.5±0.9	0.00±0.21
A-NM-3	166.9	26.29	7.2±1	2.1±0.3	2.2±0.6	2.63±0.22
A-NM-4	162.3	26.31	7.0±3	1.8±0.6	2.0±0.9	0.69±0.29
B-metal (>230 μm)	15.2	744.6	0.0233±2	−3.57±0.16		0.04±0.08
B-metal (40–230 μm)	8.11	740.9	0.0125±1	−3.18±0.19		−0.12±0.15
B-NM	183.0	18.86	11.06±8	3.7±0.7	4.0±1.1	0.55±0.48
C-WR	143.6	198.9	0.827±1	−2.79±0.26		−0.14±0.18
ALH84069 (H5)						
Metal (40–150 μm)	13.9	687.0	0.0231±2	−2.82±0.19		0.10±0.15
				−3.20±0.26		0.13±0.18
Mean				−3.01±0.53		0.12±0.06
Metal (>150 μm)	17.4	697.8	0.0284±2	−3.14±0.20		−0.05±0.13
				−3.18±0.18		0.07±0.13
				−3.20±0.17		0.01±0.10
				−2.85±0.15		0.22±0.13
Mean				−3.08±0.39		0.10±0.21
NM-1	239.2	5.35	47.4±3	25.3±0.7	32.5±6.1	−0.41±0.55
NM-2	151.6	7.48	20.8±2	9.6±0.8	12.6±3.1	−0.16±0.47
NM-3	139.3	11.58	12.0±1	4.3±0.5	5.4±1.3	−0.39±0.48
Estacado (H6)						
Metal (>150 μm)	9.64	826.1	0.01331±9	−2.98±0.21		−0.13±0.12
				−2.98±0.16		−0.08±0.12
				−3.03±0.16		−0.12±0.11
				−2.82±0.19		−0.02±0.12
				−2.72±0.15		−0.02±0.10
Mean				−2.90±0.26		−0.07±0.10
NM-1	148.5	10.5	16.2±1	4.8±1.0	5.1±1.1	−1.15±0.48
NM-2	134.3	21.1	7.27±5	1.1±0.5	1.6±0.5	2.44±0.34
Kernouvé (H6)						
Metal (40–500 μm)	1.94	926	0.00238±2	−2.86±0.19		−0.17±0.16
				−3.04±0.24		−0.12±0.14
Mean				−2.95±0.26		−0.15±0.07
Metal (>500 μm)	0.31	857	0.000415±3	−3.04±0.20		−0.13±0.14
				−2.72±0.18		−0.02±0.14
				−2.85±0.21		0.03±0.15
Mean				−2.87±0.32		−0.04±0.16
NM-1	175.9	3.9	51.0±4	23.1±0.7	25.7±2.3	−0.10±0.30
NM-2	125.7	13.3	10.8±1	2.7±0.8	2.9±1.1	−0.84±0.55
Whole-rock	141.3	183.4	0.878±7	−2.66±0.22		−0.14±0.14
				−2.41±0.20		−0.16±0.17
				−2.53±0.15		−0.01±0.10
Mean				−2.53±0.26		−0.10±0.16

NM = non-magnetic fraction. The quoted 2σ uncertainties for ^{180}Hf/^{184}W refer to the last significant digits. The quoted 2σ uncertainties for the measured ε^{182}W and ε^{183}W are standard errors of the individual mass spectrometric runs and those for the corrected ε^{182}W were calculated by propagating the external reproducibility of the isotope measurements and a 50% uncertainty on the blank correction.
The meteorites are from the following collections: Ste. Marguerite (MNHN); Richardton-A (USNM); Richardton-B (MNHN); Richardton-C (Senckenbergmuseum Frankfurt); ALH 84069 (NASA); Kernouvé (ETH); Estacado (BM).

~0.8 ε^{182}W (2 SD). This is similar to the within-run statistics obtained for the measurements of the W-poor NM fractions (Table 1), which for these samples is used as the uncertainty for the measured $^{182}W/^{184}W$. Note that the major source of uncertainty in the $^{182}W/^{184}W$ of the W-poor NM fractions is the blank correction (see below and Table 1).

The accuracy of the measurements was monitored by analyzing several carbonaceous chondrites, which all yielded the previously determined value of −1.9±0.1 ε^{182}W (Kleine et al., 2004a). Furthermore, $^{183}W/^{184}W$ ratios were used as a monitor for accurate measurements and agree for most samples to within ±0.2 ε units with the terrestrial value (Table 1). Elevated $^{183}W/^{184}W$ ratios for two NM fractions of the Richardton meteorite are attributed to an organic interference on mass 183 that was successfully removed for all other samples by treatment with HNO_3–H_2O_2. Elevated measured $^{183}W/^{184}W$ ratios have been observed before for W isotope measurements of some eucrites and carbonaceous chondrites and for these samples the $^{182}W/^{184}W$ ratio normalized to $^{186}W/^{184}W = 0.96727$ agrees with $^{182}W/^{184}W$ ratios for other eucrites and carbonaceous chondrites, respectively (Kleine et al., 2004a). This indicates that only ^{183}W is affected, such that for the two NM fractions from Richardton with elevated measured $^{183}W/^{184}W$ the reported ε^{182}W values were calculated from the $^{182}W/^{184}W$ ratio normalized to $^{186}W/^{184}W$. Note, that the ε^{182}W values thus obtained are consistent with the Hf–W data for the other fractions of Richardton and also with Hf–W data for the other H5 chondrite ALH84069 (i.e., all fractions plot on one well-defined isochron).

3. Results

The Hf and W concentrations and the W isotope composition of metals, whole-rocks and non-magnetic fractions analyzed for this study are given in Table 1. The H chondrite metals have W concentrations ranging from ~660 to ~926 ppb, consistent with previously published results (Rambaldi, 1976; Kong and Ebihara, 1996; Humayun and Campbell, 2002). These W concentrations are substantially higher than those reported for metals from unequilibrated H chondrites (Rambaldi, 1976; Kong and Ebihara, 1996; Humayun and Campbell, 2002). The $^{182}W/^{184}W$ ratios of the H chondrite metals are indistinguishable from each other but appear to increase slightly with metamorphic grade from −3.2 for H4 chondrites to −2.9 ε^{182}W for H6 chondrites. Some of the Richardton metals do not follow this trend and have ε^{182}W values as low as −3.57±0.16. Note that given an external reproducibility of ~0.3–0.4 ε units for the W isotope measurements, the $^{182}W/^{184}W$ of this sample is not distinguishable from those of the other H chondrite metals. The various NM fractions have low W contents between ~4 and ~26 ppb and Hf contents ranging from ~125 to ~239 ppb, resulting in high $^{180}Hf/^{184}W$ ratios from ~7 to ~51 and elevated $^{182}W/^{184}W$ ratios from ~2 to ~33 ε^{182}W (Table 1).

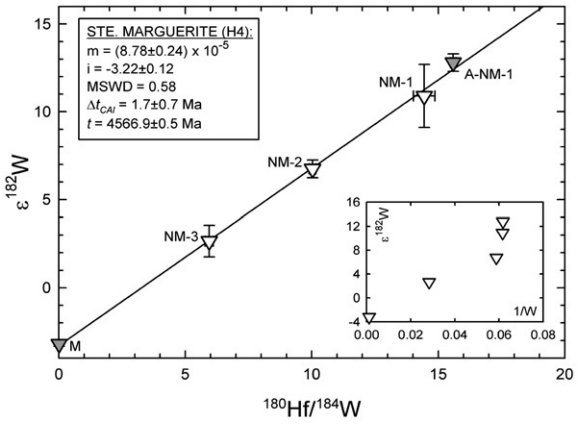

Fig. 1. ε^{182}W versus $^{180}Hf/^{184}W$ for Ste. Marguerite. Data shown with open symbols are from Kleine et al. (2002), those with filled symbols from this study. m = initial $^{182}Hf/^{180}Hf$, i = initial ε^{182}W. Regressions are calculated using the model 1 fit of IsoPlot (Ludwig, 1991). Details regarding the calculation of ages are given in the text. Δt_{CAI} is the formation interval relative to CAIs; the absolute age t is calculated relative to the angrites D'Orbigny and Sahara 99555 (see text).

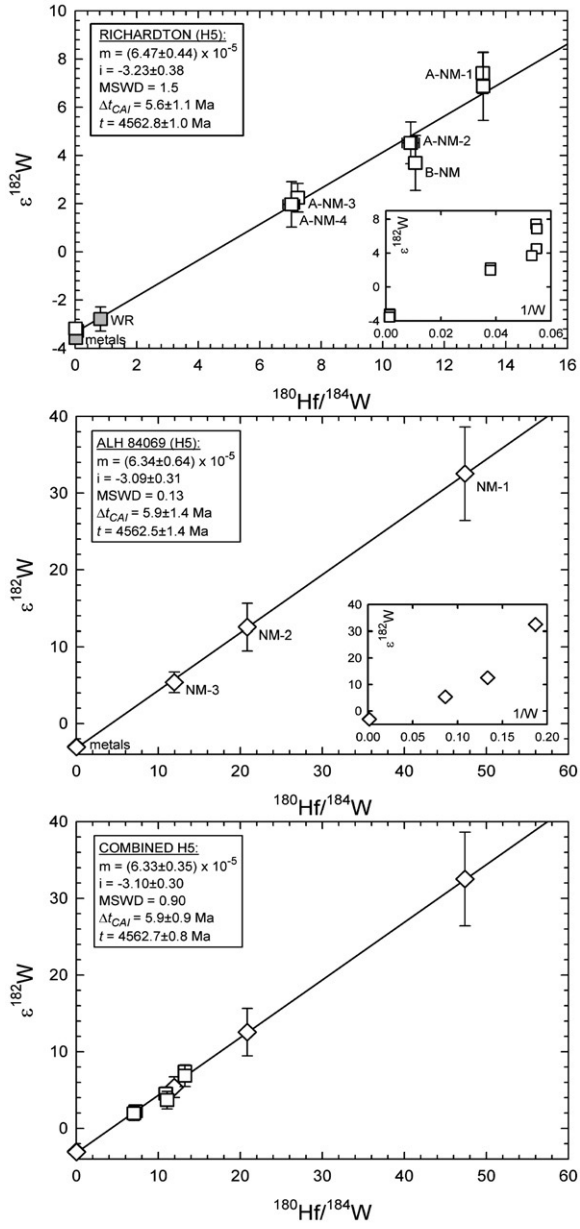

Fig. 2. ε^{182}W versus $^{180}Hf/^{184}W$ for H5 chondrites Richardton and ALH84069. m = initial $^{182}Hf/^{180}Hf$, i = initial ε^{182}W. Regressions are calculated using the model 1 fit of IsoPlot (Ludwig, 1991). Details regarding the calculation of ages are given in the text. Data shown as filled grey symbols (Richardton whole-rock and coarse-grained metal fractions) were not included in the regression and are not shown in the isochron plot for the combined H5 chondrites. Δt_{CAI} is the formation interval relative to CAIs; the absolute age t is calculated relative to the angrites D'Orbigny and Sahara 99555 (see text).

Owing to the low W contents and radiogenic $^{182}W/^{184}W$ of the NM fractions, the major source of uncertainty in the ages is the blank correction, which is significant for some of the NM fractions. Typically the blank corrections ranged from <1 to ~3 ε^{182}W. The NM-1 fraction of ALH 84069 required a larger correction of ~7 ε^{182}W, reflecting a higher W blank, which was caused by the use of insufficiently clean acetic acid (Table 1). In spite of this large correction the Hf–W data for the NM-1 fraction from ALH 84069 are consistent with the Hf–W data for its other fractions that did not require such large corrections.

As shown in Figs. 1–3, the $^{180}Hf/^{184}W$ ratios and ε^{182}W values correlate for each of the analyzed H chondrites, such that precise

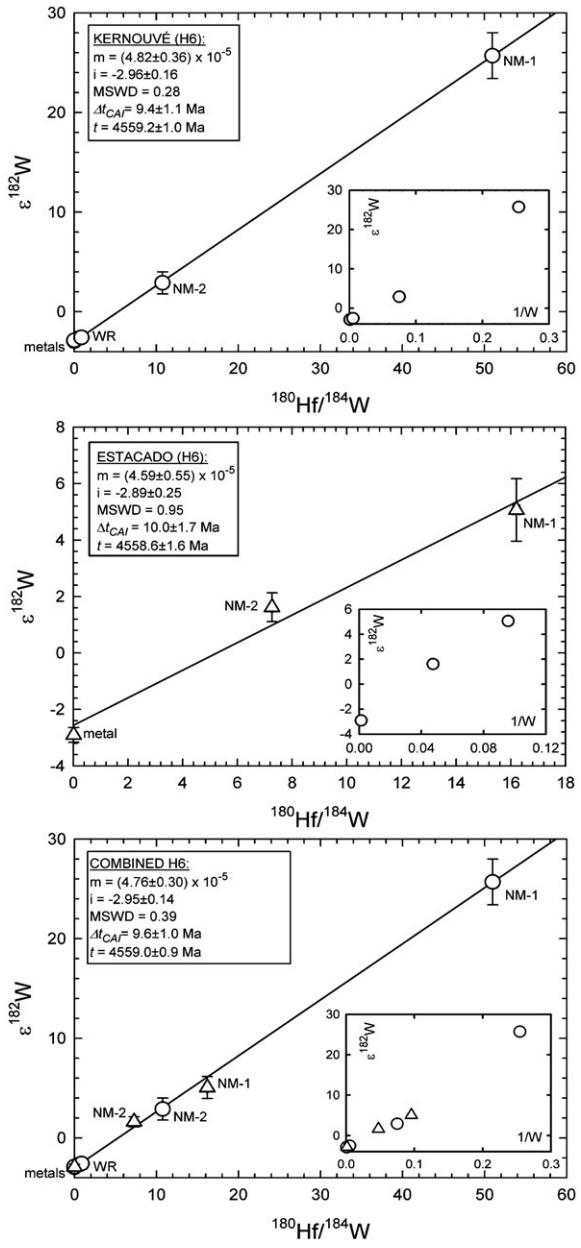

Fig. 3. $\varepsilon^{182}W$ versus $^{180}Hf/^{184}W$ for H6 chondrites Kernouvé and Estacado. m = initial $^{182}Hf/^{180}Hf$, i = initial $\varepsilon^{182}W$. Regressions are calculated using the model 1 fit of IsoPlot (Ludwig, 1991). Details regarding the calculation of ages are given in the text. Δt_{CAI} is the formation interval relative to CAIs; the absolute age t is calculated relative to the angrites D'Orbigny and Sahara 99555 (see text).

isochrons could be obtained (MSWD < 1 in most cases). The uncertainties on the slopes of the isochrons are better than ~7% in most cases, resulting in uncertainties for the ages on the order of ~1 Ma. Only for Estacado the isochron has a higher uncertainty of ~12%, resulting in an uncertainty of ±1.7 Ma.

For Richardton the scatter on the isochron is slightly larger compared to the other H chondrites, indicating a slight disturbance of the Hf–W system. A regression including all the Richardton data yields a precise isochron (MSWD = 1.2) corresponding to an initial $^{182}Hf/^{180}Hf$ of $(6.60 \pm 0.35) \times 10^{-5}$ and an initial $\varepsilon^{182}W$ of −3.39 ±0.17. This initial $\varepsilon^{182}W$ is indistinguishable from the initial $\varepsilon^{182}W$ of Allende CAIs of −3.30±0.12 (Burkhardt et al., submitted for publication) and corresponds to a W model age of −2±4 Ma (using the W isotope composition of Kernouvé as a reference), inconsistent with the age obtained from the initial $^{182}Hf/^{180}Hf$ of the Richardton isochron. Compared to the coarse-grained metal, the fine-grained Richardton metal has a slightly higher $\varepsilon^{182}W$ value, which is identical to the $^{182}W/^{184}W$ of the ALH84069 metal and also consistent with the trend of slightly increasing $\varepsilon^{182}W$ values defined by the other H chondrite metals (see Section 4.5). The model age of the fine-grained Richardton metal is 3±5 Ma, consistent with the isochron age of 5.6±1.1 Ma. This indicates that the $^{182}W/^{184}W$ ratio of the coarse-grained Richardton metal has been displaced to too low values and yields spurious ages. This has probably also affected the measured $^{182}W/^{184}W$ of the Richardton whole-rock, which is slightly displaced to lower $\varepsilon^{182}W$ values compared to the Kernouvé whole-rock (Table 1) and other H chondrite whole-rocks (Kleine et al., 2007). The origin of these low $\varepsilon^{182}W$ values remains enigmatic but could be related to the incorporation of irradiated metals with low $\varepsilon^{182}W$ values, as has been observed for many iron meteorites (Kleine et al., 2005a). However, to our knowledge there is no other evidence for the presence of such metal in Richardton. Note that this has no effect on the interpretation of the Hf–W age for Richardton, which is obtained from the slope of the isochron. This remains unchanged regardless of whether the two metal fractions with low $\varepsilon^{182}W$ and the whole-rock were included in the isochron regressions. Excluding these fractions from the regression yields a well-defined isochron (MSWD = 1.5) with an initial $^{182}Hf/^{180}Hf$ of $(6.47 \pm 0.44) \times 10^{-5}$ and initial $\varepsilon^{182}W = -3.23 \pm 0.38$ (Fig. 2).

4. Discussion

4.1. Hf–W isochron ages for H chondrites

To define an isochron the minerals of an H chondrite must once have been in W isotope equilibrium, i.e., they must have had the same W isotope composition initially. Given that the H chondrite fractions were obtained mainly based on their magnetic susceptibility, the correlation of $\varepsilon^{182}W$ with $^{180}Hf/^{184}W$ could potentially represent a mixing line between W-rich metal and virtually W-free silicates. Such a mixing line would have no chronological significance if the two

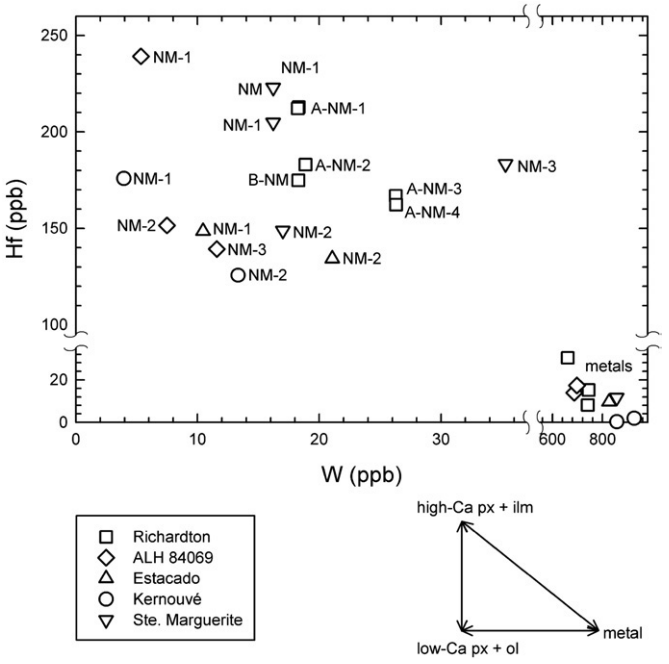

Fig. 4. Hf versus W contents for the different fractions of the analyzed H chondrites. Data for some of the NM (non-magnetic) fractions from Ste. Marguerite are from Kleine et al. (2002). The Hf and W concentrations in the coexisting phases of these H chondrites are not colinear, indicating that presence of at least three independent components for Hf and W among the coexisting phases. These components are high-Ca pyroxene + ilmenite, olivine + low-Ca pyroxene, and metal.

endmembers had different initial $^{182}W/^{184}W$ ratios. However, as shown in Fig. 4, the variations in $^{180}Hf/^{184}W$ ratios among the analyzed H chondrite fractions require the presence of at least three independent components for Hf and W among the coexisting phases. The major host of W is metal, which constitutes one component. The major hosts of Hf are high-Ca pyroxene and ilmenite (Righter and Shearer, 2003) and since no pure high-Ca pyroxene and ilmenite separates could be obtained these two phases are considered together as one component. The third component encompasses olivine and low-Ca pyroxene and is characterized by low Hf and W contents. These two minerals are considered as one component because no pure olivine and low-Ca pyroxene separates were obtained. Both olivine and low-Ca pyroxene are not capable of incorporating significant amounts of either Hf or W (Righter and Shearer, 2003), such that their presence mainly causes dilution of the high Hf content of high-Ca pyroxene and ilmenite. Given that high-Ca pyroxene, ilmenite, olivine, and low-Ca pyroxene have similar and low W contents, the slightly higher W contents of the NM-3 and -4 fractions compared to the NM-1 and -2 fractions of the same meteorite most likely reflect the presence of some metal in the NM-3 and -4 fractions.

The presence of at least three independent components with regard to Hf and W among the coexisting phases of H chondrites reveals that the correlation between $\varepsilon^{182}W$ and $^{180}Hf/^{184}W$ observed for the fractions of each of the H chondrites cannot reflect simple binary mixing between W-rich metal and virtually W-free silicates. This is also apparent from plots of $\varepsilon^{182}W$ vs. 1/W, in which binary mixtures form straight lines. This is not the case for any of the meteorites investigated here, such that the linear correlations in the $\varepsilon^{182}W$ vs. $^{180}Hf/^{184}W$ plots cannot be mixing lines (for the H6 chondrites the data seem to plot on straight lines but in the case of Kernouvé the MSWD of this $\varepsilon^{182}W$ vs. 1/W line is 4.5 instead of 0.28 for the isochron). Each of the fractions, therefore, evolved to radiogenic $\varepsilon^{182}W$ according to their $^{180}Hf/^{184}W$. Hence, the Hf–W data for the H chondrite fractions define isochrons and can be interpreted to have chronological significance.

Relative Hf–W ages (or formation intervals), Δt_{CAI}, are calculated from the initial $^{182}Hf/^{180}Hf$ ratios obtained from the slopes of the isochrons relative to an initial $^{182}Hf/^{180}Hf = (1.003 \pm 0.045) \times 10^{-4}$ for CAIs and refer to the time of Hf–W closure in a sample elapsed since crystallization of type B CAIs (Burkhardt et al., submitted for publication). With increasing metamorphic grade, the Hf–W ages of the H chondrites become increasingly younger and range from $\Delta t_{CAI} = 1.7 \pm 0.7$ Ma for the H4 chondrite Ste. Marguerite to $\Delta t_{CAI} = 9.6 \pm 1.0$ Ma for the H6 chondrites Kernouvé and Estacado. The Hf–W ages for the H5 chondrites Richardton and ALH 84069 are intermediate between the ages for the H4 and H6 chondrites and are $\Delta t_{CAI} = 5.9 \pm 0.9$ Ma.

The comparison of relative Hf–W ages and absolute Pb–Pb ages requires conversion of Hf–W formation intervals to absolute ages, which in turn requires knowledge of the initial $^{182}Hf/^{180}Hf$ and the absolute age of Hf–W closure in a sample. Due to differences in closure temperatures of different chronometers, the ideal samples to obtain such information are angrites because (i) they cooled rapidly, such that differences in closure temperatures do not result in resolvable age differences, and (ii) they exhibit high U/Pb ratios, such that precise Pb–Pb ages are available (Lugmair and Galer, 1992; Amelin, 2008). The most precise Pb–Pb age for the angrites D'Orbigny is 4564.42 ± 0.12 Ma (Amelin, 2008). For the angrite Sahara 99555, the earlier reported Pb–Pb age of 4566.18 ± 0.14 Ma (Baker et al., 2005) has now been revised and two identical ages of 4564.58 ± 0.14 and 4564.86 ± 0.38 Ma, obtained using different techniques for the removal of Pb contamination, were reported (Connelly et al., 2008). Mineral separates from D'Orbigny and Sahara 99555 plot on one well-defined Hf–W isochron (MSWD = 1.4) yielding an initial $^{182}Hf/^{180}Hf$ of $(7.31 \pm 0.16) \times 10^{-5}$ [recalculated from the Hf–W data reported in Markowski et al. (2007) and using the model 1 fit of IsoPlot], consistent with identical Pb–Pb ages for these two angrites. Here we calculate absolute Hf–W ages relative to an initial $^{182}Hf/^{180}Hf = (7.31 \pm 0.16) \times 10^{-5}$ at 4564.50 ± 0.23 Ma (i.e., the average of the aforementioned Pb–Pb ages for D'Orbigny and the more precise age for Sahara 99555). Identical results are obtained if absolute Hf–W ages were calculated relative to D'Orbigny only or Sahara 99555 only.

This approach for calculating absolute Hf–W ages is based on the assumption that the Pb–Pb ages for D'Orbigny and Sahara 99555 accurately date the crystallization of these rocks. Several Pb–Pb studies on angrites, however, reported Pb–Pb ages for the same angrite that are distinct outside of the reported age uncertainties (Baker et al., 2005; Amelin, 2008; Connelly et al., 2008). Nevertheless, given that two groups obtained identical high-precision Pb–Pb ages for the angrites D'Orbigny and Sahara 99555 (Amelin, 2008; Connelly et al., 2008), these ages appear reliable and their use as reference ages for Hf–W chronometry justified. Moreover, Hf–W ages for two other angrites (Kleine et al., 2008) are consistent with their Pb–Pb ages (Amelin and Irving, 2007), indicating that the intercalibration of Hf–W and Pb–Pb ages provides reliable results.

4.2. Closure temperature for the Hf–W system in equilibrated H chondrites

To evaluate the significance of the Hf–W ages for constraining the thermal evolution of meteorite parent bodies, it is necessary to know the closure temperature for W diffusion in the appropriate silicate-metal mixture. In H chondrites, the major hosts of radiogenic ^{182}W are high-Ca pyroxene and ilmenite and each of these minerals might have its distinct Hf–W closure temperature. In slowly cooled metamorphic rocks such as H chondrites, one of these two minerals may have stayed open while the other had already closed. This would result in scatter on the isochron but this is not observed for the data presented here. This indicates that there are no significant differences in the Hf–W closure temperatures of high-Ca pyroxene and ilmenite in H chondrites, given that the variable Hf contents in the different NM fractions most likely reflect different proportions of ilmenite and high-Ca pyroxene in these fractions.

There are no experimental data available for diffusion of W in high-Ca pyroxene or ilmenite that would allow calculation of the closure temperature as a function of effective grain size and cooling rate. Based on the comparison of Hf–W ages for eucrite metals with Pb–Pb ages for the host eucrites, Kleine et al. (2005b) estimated the closure temperature of the Hf–W system in basaltic eucrites to be at least ~600 °C. Here we estimate the closure temperature of the Hf–W system by modeling the diffusion behavior of W in high-Ca pyroxenes and test these results by comparison to Pb–Pb ages for chondrites.

The diffusion behavior of W in high-Ca pyroxene was evaluated by (i) using the model presented by Van Orman et al. (2001) to estimate the diffusion parameters for W in high-Ca pyroxene and by (ii) modeling the diffusion behavior of W in a high-Ca pyroxene-metal system. Tungsten is assumed to have a charge of +4, an ionic radius of 0.066 nm (Shannon, 1976) and is assumed to reside on the 6-fold coordinated M1 site in high-Ca pyroxene, which has an ideal radius of 0.072 nm and metal–oxygen bond length of 0.22 nm. Assuming that the Van Orman et al. (2001) model applies to cations that occupy the M1 site – which appears reasonable since the model predicts diffusion coefficients for Fe^{2+} on the M1 site that are in good agreement with experimental data (Azough and Freer, 2000) – gives an activation energy estimate of 453 kJ/mol and a pre-exponential factor of 9.53×10^{-5} m^2/s.

Simultaneous production and diffusive exchange of radiogenic W between high-Ca pyroxene and metal was simulated numerically using the model of Van Orman et al. (2006). We chose to use this numerical model rather than the analytical models for closure temperature presented by Dodson (1973) and Ganguly and Tirone (2001) because the analytical models make several assumptions that do not necessarily apply to the cases considered here. For example, the

Dodson (1973) and Ganguly and Tirone (2001) models assume (i) an infinite sink for radiogenic daughters (which is a valid assumption in the case of H chondrites); (ii) a decay time that is very long compared to the cooling time (which might not be valid for short-lived chronometers); and (iii) that heating at peak metamorphic conditions was sufficient to homogenize the high-Ca pyroxene. The numerical model used here does not rely on these assumptions, and is thus a more realistic model for the production and exchange of radiogenic daughters in short-lived isotope systems. As will be shown below, the assumption that peak metamorphic conditions were sufficient to reset the Hf–W system is not valid in the case of the H4 chondrites. Assessing the effects that metamorphism had on the Hf–W system in H4 chondrites therefore requires a model that can simulate the prograde path, such as the one used here.

In the model, exchange of radiogenic W is controlled by diffusion within spherical high-Ca pyroxene grains, which maintain partitioning equilibrium with metal at their surfaces. Because diffusion in Fe–Ni alloys is many orders of magnitude more rapid than in high-Ca pyroxene (Watson and Watson, 2003), the metal is assumed to remain homogeneous throughout the simulation. In most simulations, ^{182}W is assumed to be distributed in chemical and isotopic equilibrium between the high-Ca pyroxene and metal at the peak temperature. However, we also performed simulations, described below as applied to H4 and H5 chondrites, in which the sample had experienced a cold pre-history, during which radiogenic W was not transferred from the high-Ca pyroxene to the metal.

The system is assumed to cool linearly with time from the peak temperature, and the final age is calculated based on the integrated concentrations of ^{182}W in the high-Ca pyroxene and the metal resulting from the decay of ^{182}Hf. This age corresponds to a particular temperature along the cooling path, which is by definition the closure temperature of the system. The cooling time from peak temperatures to temperatures at which diffusive exchange becomes negligible is ~10 Ma, which is similar to the ^{182}Hf half-life. In the cases considered here, diffusive exchange ceased before ^{182}Hf had completely decayed, such that while the system remains open to exchange, the decay of ^{182}Hf is significant.

The closure temperature estimates shown in Fig. 5 assume an initial temperature of 1000 °C. This temperature provides an upper limit for the peak temperature of H6 chondrites because at ~1000 °C melting in the FeNi–FeS system begins but the texture of H6 chondrites reveals that such melting did not occur. Assuming an initial temperature of ~1000 °C appears reasonable because temperature estimates for H6 chondrites using the two-pyroxene thermometer (Lindsley, 1983) yield a temperature range of 865–926 °C (Slater-Reynolds and McSween, 2005), only slightly below 1000 °C. The peak metamorphic temperatures for H4–5 chondrites are less well constrained, mainly because in these rocks the pyroxenes are not completely equilibrated, such that two-pyroxene thermometry cannot be applied. Based on temperature estimates for type 3 (obtained from Ni profiles in taenite) and type 6 chondrites, Dodd (1981) estimated the peak temperatures for type 4 and type 5 chondrites to 600–700 °C and 700–750 °C, respectively. In more recent studies olivine–spinel thermometry was used to determine temperatures for type 4–6 chondrites and the results for H4–6 chondrites tightly cluster between 675 and 750 °C (Wlotzka, 2005; Kessel et al., 2007). These temperatures provide a lower limit for the peak temperatures and the tight cluster of olivine–spinel temperatures suggest that peak temperatures for H4–6 chondrites were not very different (Wlotzka, 2005; Kessel et al., 2007).

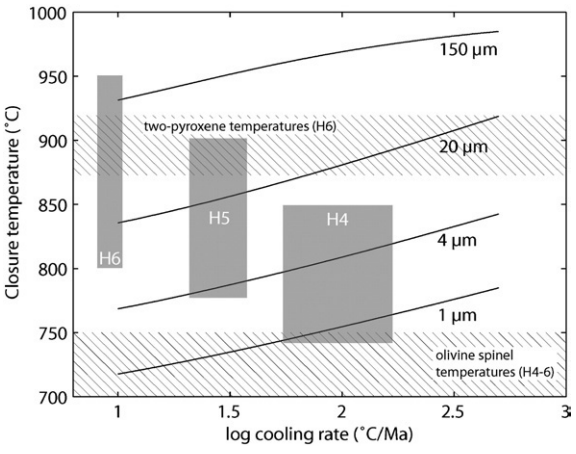

Fig. 5. Closure temperature of the Hf–W system as function of grain diameter and cooling rate. The assumed starting temperature is 1000 °C. Details regarding the calculations are given in the text. The dashed areas indicate two-pyroxene and olivine–spinel temperatures for H chondrites. The grey boxes indicate typical cooling rates and grain sizes of high-Ca pyroxene for each of the petrologic types of H chondrites.

Fig. 5 shows closure temperatures calculated as a function of cooling rate, for an initial temperature of 1000 °C and four different high-Ca pyroxene grain diameters between 1 and 150 μm. The high-Ca pyroxene/metal ratio in these simulations is 0.5 and the high-Ca pyroxene/metal partition coefficient for W is 0.01 (Walter and Thibault, 1995), but the results are not sensitive to variations in these parameters unless the high-Ca pyroxene/metal ratio and/or partition coefficient become much larger.

Fig. 5 reveals that the closure temperature of the Hf–W system in H chondrites is strongly dependent on the grain size of the high-Ca pyroxenes, particularly for grain sizes below ~20 μm. As a consequence, T_c increases from H4 to H6 chondrites because the grain sizes of high-Ca pyroxenes increase. In H6 chondrites, the high-Ca pyroxenes are 5–30 μm in diameter, whereas in H5 chondrites they are 2–5 μm but can also be larger (Huss et al., 2006). In H4 chondrites, high-Ca pyroxene microcrystallites may have diameters of less than 1 μm but high-Ca pyroxenes also occur as euhedral grains of less than ~10 μm in the mesostasis and form rims around olivine and low-Ca pyroxene that are ~10–20 μm across (Huss et al., 2006; C. Alexander and J. Grossmann, pers. comm. 2007). Using these grain sizes the following values for T_c are obtained (Fig. 5): ~800–875 °C (H6); ~750–850 °C (H5); ~725–850 °C (H4). However, these temperature estimates assume that high-Ca pyroxene and metal are always in direct contact but given that high-Ca pyroxene is only a minor constituent in H chondrites this will probably not be the case. A more realistic approach is to assume that the high-Ca pyroxene grains are surrounded and sometimes even enclosed by large olivine and low-Ca pyroxene grains (with grain diameters between 20 and 200 μm). These grains would constitute a barrier for W diffusion from the high-Ca pyroxene to the metal and the estimates for T_c presented above are then lower limits.

A higher limit for T_c is given by the peak temperature of H6 chondrites that must have been below ~1000 °C and above the two-pyroxene temperature of ~900 °C (see above). It therefore is reasonable to assume that the higher limit of T_c in H6 chondrites is ~950 °C. For H5 chondrites the peak temperature probably was somewhat lower and here we assume ~900 °C. Combined with the lower limits for T_c obtained from Fig. 5 and based on the grain sizes of the high-Ca pyroxenes the following values for T_c are obtained: 875±75 °C for H6 chondrites and 825±75 °C for H5 chondrites.

The Hf–W closure temperature for H4 chondrites is more difficult to estimate than those for H5 and H6 chondrites because the peak temperature in H4 chondrites as well as the host phase(s) of radiogenic ^{182}W and its grain size(s) in H3 chondrites are less well constrained. In type 3 chondrites, Hf is enriched in the mesostasis (and high-Ca pyroxenes therein) of chondrules and in high-Ca rims on olivine and low-Ca pyroxene grains in chondrules (Alexander, 1994). Tungsten most likely is concentrated in metal grains outside

chondrules and in the matrix (see below). The rate of diffusive transport of radiogenic ^{182}W from the chondrules into metal outside the chondrules is difficult to model and critically depends on the exact location of W in the chondrules and, as is evident from Fig. 5, on the high-Ca pyroxene grain size. The range in grain sizes of <1 μm to ~10 μm corresponds to a range in T_c of ~100 °C (Fig. 5). In addition, the rate of W diffusion depends on the grain sizes of olivine and low-Ca pyroxene inside the chondrules, which control how many grain boundary paths there are between the high-Ca pyroxenes and the metals. A lower limit for T_c may be obtained by assuming that radiogenic ^{182}W is located inside ~0.1 μm high-Ca pyroxene microcrystallites, which are in direct contact to metals outside the chondrules. In this model, a closure temperature of ~700 °C is calculated. The true value for T_c will be significantly higher because larger high-Ca pyroxenes are present and the high-Ca pyroxenes inside the chondrules and metal grains outside the chondrules will mostly not be in direct contact. A higher limit for T_c may be obtained by assuming that all high-Ca pyroxenes have grain sizes of ~10 μm, in which case the closure temperature will be ~850 °C (Fig. 5). Given that many of the high-Ca pyroxene grains in H4 chondrites have sizes larger than ~1 μm, T_c will probably be higher than ~750 °C (Fig. 5) and the best estimate for T_c in H4 chondrites then is 800±50 °C.

The comparison of the Hf–W ages and other ages provides a test for the validity of the above closure temperature estimates. For Ste. Marguerite, Kernouvé and Estacado the Hf–W ages are the oldest radioisotopic ages reported for these meteorites so far, for Richardton the Hf–W and Pb–Pb chondrule ages are indistinguishable (Table 2). The most reliable approach for estimating closure temperatures by age comparison uses slowly cooled samples because then differences in closure temperatures among different isotope systems and minerals will result in resolvable age differences. The Hf–W age for Kernouvé is ~23 Ma older than Pb–Pb whole-rock and pyroxene ages (Göpel et al., 1994; Bouvier et al., 2007) for this meteorite and the Hf–W age for Estacado is ~30 Ma older than a Pb–Pb chondrule age (Blinova et al., 2007) (Table 2). This indicates that the Hf–W closure temperature must be well above the closure temperature for Pb diffusion in pyroxenes (Cherniak, 1998; Amelin et al., 2005), consistent with the observation that Hf–W ages for eucrite metals are older than Pb–Pb ages for their host eucrites (Kleine et al., 2005b). The closure temperature for Pb diffusion in pyroxenes in H6 chondrites was estimated to be 780±100 °C for grain sizes of 20–200 μm (Amelin et al., 2005), which is indistinguishable from but appears to be slightly lower than our estimate for the Hf–W closure temperature in H6 chondrites of 875±75 °C. This indicates that the closure temperature estimates for the Hf–W system presented here are reasonable. It is important to note that the Pb closure temperature for pyroxenes in H chondrites might be lower than 780±100 °C because in these samples the grain sizes of the high-Ca pyroxene (Huss et al., 2006) are smaller than the 20–200 μm range used in the calculation by Amelin et al. (2005). High-Ca pyroxenes are probably an important host of U among the silicate minerals of H chondrites because U fits much better into the M2 (i.e., Ca) site of pyroxenes and should therefore be enriched in high-Ca relative to low-Ca pyroxene. For grain sizes of 5–30 μm the closure temperature for Pb diffusion ranges from ~650 °C to ~780 °C and decreases to temperatures as low as ~550 °C for grain sizes of ~1 μm. As for the Hf–W system these closure temperature estimates probably are lower limits because they do not take into account the effects of large olivine and low-Ca pyroxenes (e.g., as barriers for Pb diffusion). However, these calculations reveal that the Hf–W closure temperature in H6 chondrites is distinctly higher than the U–Pb closure temperature in pyroxenes, consistent with the well-resolved differences in Hf–W and Pb–Pb ages for Kernouvé and Estacado.

Table 2
Compilation of radiometric ages for selected H chondrites (in Ma)

Sample	Minerals	Age (Ma)±2σ	T_c (°C)	System	References
Ste. Marguerite	metal-silicate	4566.9±0.5	800±50	^{182}Hf–^{182}W	this study
	whole-rock, chondrules	4564.4±3.4	650±100	^{207}Pb–^{206}Pb	(3,4)
	phosphates	4562.7±0.6	477±100	^{207}Pb–^{206}Pb	(4)
Richardton	metal-silicate	4563.0±0.9	825±75	^{182}Hf–^{182}W	this study
	chondrules	4562.7±1.7	725±100	^{207}Pb–^{206}Pb	(1)
	phosphates	4550.7±2.6	477±100	^{207}Pb–^{206}Pb	(1,4)
Estacado	metal-silicate	4558.6±1.6	875±75	^{182}Hf–^{182}W	this study
	chondrules	4527.6±6.3	777±100	^{207}Pb–^{206}Pb	(2)
	phosphates	4492±15	477±100	^{207}Pb–^{206}Pb	(2)
Kernouvé	metal-silicate	4559.2±1.0	875±75	^{182}Hf–^{182}W	this study
	whole-rock; pyroxene-olivine	4536±7	777±100	^{207}Pb–^{206}Pb	(3,4)
	phosphates	4522.5±1.5	477±100	^{207}Pb–^{206}Pb	(4)

The Pb–Pb ages for whole-rocks and silicates from Ste. Marguerite and Kernouvé are averages of the ages reported in the literature. The uncertainties are calculated as standard deviations (2σ) of these ages. For estimates of the closure temperatures see text. (1) Amelin et al. (2005); (2) Blinova et al. (2007); (3) Bouvier et al. (2007); (4) Göpel et al. (1994).

4.3. Significance of the Hf–W ages

To utilize Hf–W ages for H chondrites for constraining the timescales of parent body accretion, heating and cooling it is essential to identify which "events" are being dated. In the case of metamorphic rocks such as H chondrites, these could be (i) cooling from peak metamorphic temperatures below T_c, (ii) mineral growth during metamorphism (this could take place below T_c), or (iii) a pre-metamorphic event (in the case that metamorphism was not capable of resetting the Hf–W system). The interpretation of the Hf–W ages critically depends on (i) whether heating above T_c was achieved, and (ii) how efficiently any initial W isotope heterogeneity, produced by the decay of ^{182}Hf in phases having different Hf/W, has been erased by the thermal metamorphism.

4.3.1. Hf–W age of the H4 chondrite Ste. Marguerite: timing of chondrule formation

The lower limit of the Hf–W closure temperature for H4 chondrites overlaps with the upper limit of ~750 °C of olivine–spinel temperatures determined for this chondrite group (Wlotzka, 2005; Kessel et al., 2007). Peak temperatures of H4 chondrites may be higher than the olivine–spinel temperatures but to what extent is unknown. It is therefore difficult to estimate if H4 chondrites were heated above T_c but it appears that for complete resetting of the Hf–W system heating to ~800–850 °C would be required. This is only slightly below the peak temperatures of H6 chondrites and it seems unlikely that this has been achieved. Moreover, the high olivine–spinel temperature for H4 chondrites may in part reflect an earlier high-temperature event (such as chondrule formation), in which case the peak temperatures of the H4 chondrites could be below 700 °C, consistent with temperature estimates by Dodd (1981).

To evaluate whether the Hf–W age for Ste. Marguerite reflects parent body metamorphism, we numerically simulated the diffusional exchange of W between clinopyroxene and metal using the model of Van Orman et al. (see above). In the simulation, we led a clinopyroxene-metal system evolve for 1 Ma at low temperatures, such that no diffusional exchange between clinopyroxene and metal could occur, then instantaneously heated to 800 °C and led the system cool at ~200°/Ma. The simulations indicate that such a scenario is not capable of erasing the previously accumulated radiogenic W isotope signature of the clinopyroxene. In this particular scenario, the age of the system would only shift by 0.07 Ma, i.e., if 2.7 Ma would be the time of heating, the Hf–W age would still be 1.77 Ma and, hence, almost entirely reflect the earlier event.

Two lines of evidence further suggest that the Hf–W age for Ste. Marguerite has not been reset by parent body metamorphism. First,

the Hf–W age for Ste. Marguerite of 1.7±0.7 Ma is identical to Al–Mg ages for chondrules from L and LL chondrites (Russell et al., 1996; Kita et al., 2000; Rudraswami and Goswami, 2007). Although no ages for chondrules from H chondrites are available it seems likely that H chondrules formed at the same time as L and LL chondrules, given that both L and LL chondrules have identical average Al–Mg ages of ~2 Ma (Russell et al., 1996; Kita et al., 2000; Rudraswami and Goswami, 2007). Hence, H chondrules probably formed at ~2 Ma, which is the time given by the Hf–W age for Ste. Marguerite. Second, since chondrules formed before the assembly of their host parent body, chondrule ages provide the earliest time at which assembly of and hence heating inside the parent body can have started. Thermal modeling of spherical asteroids heated by ^{26}Al decay indicate that a temperature increase to ~700 °C is unlikely to have been achieved earlier than ~1 Ma after accretion. This suggests that the 1.7±0.7 Ma Hf–W age for Ste. Marguerite could only date parent body processes if the H chondrite parent body formed much earlier than the L and LL chondrite parent bodies. However, this would imply that due to ^{26}Al heating significant parts of the H chondrite parent body would have melted and differentiated.

However, ordinary chondrite parent bodies appear to be well sampled by breccias but these do not contain any differentiated material (Scott, 2006), which would be expected if the H chondrite parent body had been partially differentiated. Based on the similar Δ^{17}O values of H chondrites and silicate inclusions from IIE iron meteorites it was suggested that IIE metal might represent the core of the H chondrite parent body (Clayton and Mayeda, 1996). However, similarity in Δ^{17}O values does not require identical parent bodies, as is evident from meteorites that derive from distinct parent bodies but have identical Δ^{17}O values (e.g., enstatite chondrites, aubrites, terrestrial and lunar rocks; IVA irons and LL chondrites).

These arguments suggest that in Ste. Marguerite metamorphism on the parent body did not result in significant diffusion of radiogenic W out of high-Ca pyroxene. However, elemental diffusion of W into metals clearly occurred. This is evident from the substantially higher W contents of metals from type 4 chondrites compared to metals from type 3 chondrites (Rambaldi, 1976; Kong and Ebihara, 1996; Humayun and Campbell, 2002). Evaluating whether this elemental transfer of W could have caused resetting of the Hf–W age critically depends on identifying the original host of the W that diffused into the metals during metamorphism of H4 chondrites. H chondrites contain ~180 ppb W (Table 1) and metals in H3 chondrites have ~300 ppb W, i.e., only ~30% of the entire W resides in the metal (assuming a metal mass fraction of 20%). In contrast, metals in H4 chondrites Ste. Marguerite have ~800 ppb W, indicating that almost all W (~90%) is located in the metals. Consequently, during metamorphism ~60% of the entire W in H chondrites must have diffused into the metals. None of the major silicate minerals in H chondrites (i.e., olivine, low-Ca pyroxene, high-Ca pyroxene) is capable of incorporating such high amounts of W (Righter and Shearer, 2003), as a consequence these minerals cannot be the original host of the W that has been mobilized during metamorphism and incorporated into the metals. Non-magnetic fractions from ordinary chondrites have Ir contents that are too high to reflect equilibrium distribution between metal and silicates (Palme et al., 1981). This suggests that ordinary chondrites contain a component with appreciable amounts of siderophile elements (including W) that cannot be separated from silicates with a hand-magnet. This phase could be tiny metal grains (that are too small to be separated with a hand-magnet) or small refractory inclusions that reside in the matrix. It is conceivable that W from these phase(s) became easily mobilized during metamorphism and diffused, probably along grain boundaries, into the metals. This W probably was not radiogenic because the Hf/W ratios in its host metal grains or refractory inclusions likely were low. For instance, the ^{182}W/^{184}W in a reservoir with ^{180}Hf/^{184}W ~ 1.7 (i.e., a value typical for CAIs) only changes by ~0.12 ε/Ma, such that the W that diffused into the metals of H4 chondrites most likely had a W isotope composition very similar to the ^{182}W/^{184}W of the H3 metal. The elemental diffusion of W from the matrix into the metals therefore most likely had no measurable effect on the ^{182}W/^{184}W of the H4 chondrite metal and hence did not affect the slope of the metal-high-Ca pyroxene isochron.

4.3.2. Hf–W ages for H5 and H6 chondrites: timing of the thermal peak

The Hf–W isochrons for the H5 and H6 chondrites investigated here are shallower than those of Ste. Marguerite, indicating that diffusion of radiogenic W from high Hf/W phases occurred in these samples. The interpretation of the Hf–W ages for the H5 and H6 chondrites critically depends on whether this diffusion completely erased any preexisting W isotope heterogeneity. To evaluate this we performed simulations similar to those for H4 chondrites. We let a high-Ca pyroxene-metal system evolve for 1 Ma at low temperatures, such that no diffusional exchange between high-Ca pyroxene and metal could occur, then instantaneously heated to 950 °C and let the system cool at 34 °C/Ma (see below). Using a 4 μm effective grain size for the high-Ca pyroxenes the system homogenizes almost as soon as cooling begins, suggesting that any initial W isotopic heterogeneity in Richardton has been largely erased by the thermal metamorphism. This is consistent with the observation that the Hf–W age for Richardton is identical to the Pb–Pb age for its chondrules. Owing to the slower diffusivity of W compared to Pb, incomplete resetting would be more pronounced for the Hf–W system than for the Pb–Pb system, such that in the case of incomplete resetting the apparent Hf–W age would be older than the apparent Pb–Pb age. The difference should increase with a decreasing degree of resetting. However, the Hf–W and Pb–Pb ages for Richardton of 4563.0±0.9 and 4562.7 ±1.7 Ma (Amelin et al., 2005), respectively, are identical, such that the effects of incomplete resetting seem to be minor or absent and both ages should date cooling from peak metamorphic temperatures. Given that H6 chondrites were heated to higher (or at least similar) peak temperatures and cooled at a slower rate, this implies that the Hf–W ages for H6 chondrites also reflect cooling below the Hf–W closure temperature.

The difference in Hf–W ages between H4 and H6 chondrites is only ~8 Ma and much shorter than intervals of ~74 Ma based on the elevated initial ^{87}Sr/^{86}Sr of phosphates from the H6 chondrite Guareña (Wasserburg et al., 1969) and ~40 Ma based on the differences in Pb–Pb ages of phosphates from Ste. Marguerite (H4) and Kernouvé (H6) (Göpel et al., 1994). Humayun and Campbell (2002) argued that the abundance and isotope composition of W in metals from ordinary chondrites of type 4, 5, and 6 was set at the same time during the prograde path, whereas other ages were interpreted as postmetamorphic cooling ages. This conclusion was based on the observation that metals from type 4, 5, and 6 have constant W/Ir ratios that are distinct from the variable W/Ir ratios observed for metals from type 3 ordinary chondrites (Humayun and Campbell, 2002). According to Humayun and Campbell (2002) this reflects termination of W diffusion (both elemental and isotopic) from silicates into metal at metamorphic conditions characteristic for type 4 chondrites. These authors further argue that the transfer of W from silicates to metal is facilitated by W reduction in the presence of C and that the major C-bearing phases in ordinary chondrites are decomposed in the earliest stages of metamorphism. As a consequence, reduction of W and its transfer from silicates into metal would no longer be possible in type 5 and 6 ordinary chondrites and Hf–W ages for type 4, 5, and 6 chondrites should be identical.

However, the Hf–W ages and closure temperature estimates presented here reveal that this is not the case and that continued diffusional exchange of W occurred in the type 5 and 6 chondrites. The much shorter Hf–W interval compared to the Rb–Sr and Pb–Pb intervals rather highlights the fact that the Hf–W system closed early and, hence, dates processes associated with the earliest evolution of the H chondrite parent body.

4.4. Constraints on the accretion and cooling history

The Hf–W ages for the H chondrites can be used to constrain the cooling history and structure of the H chondrite parent body. Temperature profiles for spherical asteroids heated by energy released from ^{26}Al decay (Carslaw and Jaeger, 1959) were calculated using parameters similar to those of Miyamoto et al. (1981) and results similar to those of Trieloff et al. (2003) were obtained (details are given in the caption of Fig. 6). The model used here is an over-simplification because it assumes instantaneous accretion and does neither include the insulating effects of a regolith (Akridge et al., 1998) nor temporal and local variations in physical and thermal parameters (e.g., changes in thermal conductivity due to a decrease in porosity) (Bennett and McSween, 1996). If accretion took place over a timescale similar to the ^{26}Al half-life, then a body starts retaining the heat produced by ^{26}Al decay before reaching its terminal mass and peak temperatures are reached earlier than estimated when assuming instantaneous accretion (Merk et al., 2002; Ghosh et al., 2003). A thick insulating regolith results in a more uniform temperature distribution in the interior, such that peak temperatures can be reached at shallower levels compared to the model used here (Akridge et al., 1998).

Nevertheless, to a first order, the thermal model presented here is useful for calculating cooling curves for individual samples that are consistent with the chronological data and for constraining the structure and thermal history of the H chondrite parent body. The calculated temperature profiles for different depth in a spherical body with a 100 km radius are shown in Fig. 6 and reveal that all chronological data combined are consistent with the simple thermal model used here: the high-temperature (>500 °C) cooling history constrained by the Hf–W ages is consistent with the low-temperature (<500 °C) cooling history as constrained earlier (Trieloff et al., 2003). For each of the samples well-defined cooling curves are obtained, suggesting that these samples cooled more or less undisturbed from their peak temperatures to less than ~100 °C. This provides evidence that at least parts of the H chondrite parent body stayed intact and were not disrupted and reassembled.

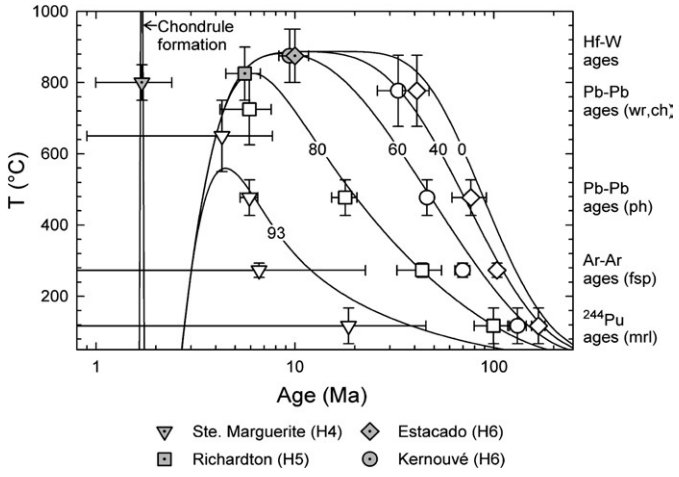

Fig. 6. Cooling curves for H chondrites. Solid lines indicate calculated temperature profiles for different depth in a spherical body with a 100 km radius. Numbers indicate distance in km from the center. We used the following parameters adapted from Miyamoto et al. (Miyamoto et al., 1981): thermal conductivity $K = 1.0$ W m^{-1} K^{-1}; thermal diffusivity $\kappa = 5.0 \times 10^{-7}$ m^2 s^{-1}; density $r = 3.2 \times 10^3$ kg m^{-3}; heat generation $A = 11.67 \times (^{26}\text{Al}/^{27}\text{Al})$ W m^{-3}; emissivity $h = 1.0$ m^{-1}. The assumed ambient temperature is $T_0 = 300$ K and the initial ^{26}Al/^{27}Al is 4.5×10^{-6}, corresponding to accretion at 2.7 Ma after CAIs. Hf–W ages and closure temperatures are from this study, all other ages are from the literature (references are given in Table 2). wr = whole-rock, ch = chondrules, ph = phosphates, fsp = feldspar, mrl = merrilite. Ar–Ar and ^{244}Pu ages are shifted by ~30 Ma due to the proposed revision in the ^{40}K decay constant (Trieloff et al., 2001; Min et al., 2003; Trieloff et al., 2003).

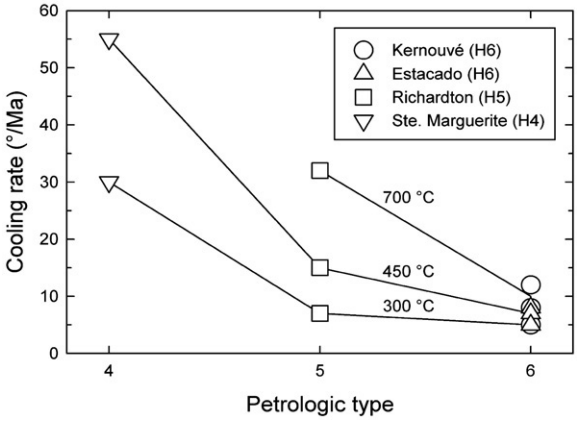

Fig. 7. Cooling rate versus petrologic type for H chondrites from this study. For both high and low temperatures there is an inverse correlation of cooling rates with petrologic type, consistent with an onion-shell structure of the H chondrite parent body. The lack of such a correlation between metallographic cooling rates and petrologic type for some H chondrites (Taylor et al., 1987) probably reflects impact-related disturbance of parts of the H chondrite parent body during the low-temperature interval (<500 °C).

Cooling rates for H chondrites can be obtained from the slope of the cooling curves. This reveals a marked decrease in cooling rates from H4 to H6 chondrites (Fig. 7). For instance, at ~700 °C the H6 chondrites Kernouvé and Estacado cooled at ~10°/Ma, whereas the H5 chondrite Richardton cooled at ~30 °C/Ma; at ~400 °C the H6 chondrites cooled at ~5 °C/Ma, Richardton at ~12 °C/Ma and the H4 chondrite Ste. Marguerite at ~50 °C/Ma. This inverse correlation of cooling rate with petrologic type is most consistent with an onion-shell structure of the H chondrite parent body. However, the lack of such a correlation between metallographic cooling rates and petrologic type for some other H chondrites suggests that in some parts of the H chondrite parent body cooling from ~500 to ~300 °C did not take place in a body with onion-shell structure (Taylor et al., 1987). The low temperature cooling history of these parts of the H chondrite parent body therefore is most readily explained by impact-related disturbance of parts of the parent body.

Although the Hf–W data do not provide direct age constraints on the timescales of accretion of the H chondrite parent body – because none of the Hf–W ages directly relates to the process of accretion – they can nevertheless be used to obtain minimum and maximum ages for accretion. Accretion could not have started before chondrule formation at 1.7 ± 0.7 Ma, as given by the Hf–W age for Ste. Marguerite. The end of accretion is less well constrained but the Hf–W age for H5 chondrites of $\Delta t_{CAI} = 5.9 \pm 0.9$ Ma as well as the 4562.7 ± 0.6 Ma Pb–Pb age for phosphates from Ste. Marguerite (H4) indicate that H4 and H5 chondrites had already reached their thermal peak and cooled below ~800 °C (H5) and ~450 °C (H4), respectively, as early as ~6 Ma after CAI formation. It therefore is unlikely that significant accretion occurred later than ~6 Ma. Additional constraints on the duration of accretion are provided by the distinct sizes and chemical properties of chondrules from each chondrite group. In a turbulent solar nebula, chondrules would be efficiently mixed on short timescales (Cuzzi et al., 2005), such that a characteristic population of chondrules with its distinct size distribution and chemical composition could only be preserved, if this chondrule population is accreted into larger bodies soon after chondrule formation. This was quantified by Alexander (2005), who estimated that material in a 1 AU wide area could be mixed within less than ~0.5 Ma. Since asteroid feeding zones probably were smaller, these mixing times become even shorter. If these estimates are correct, chondrite accretion must have occurred almost instantaneously after chondrule formation (Alexander, 2005). This

does not necessarily imply that the entire H chondrite parent body was accreted at 1.7±0.7 Ma (or soon after). It might also be possible that several smaller objects formed at that time and were combined later to the H chondrite parent body. However, as argued above, this process was largely complete by ~6 Ma after CAI formation at the latest.

There are two endmember interpretations for the Hf–W age of H6 chondrites. First, this age could reflect cooling from the thermal peak of ~950 °C below T_c=875±75 °C for H6 chondrites. In this case, the Hf–W age would almost reflect the time when cooling from the thermal peak started. Alternatively, temperatures inside the H chondrite parent body remained at their peak for longer but T_c increased due to grain coarsening and the Hf–W system closed although cooling had not yet started. In this case, metamorphic temperatures could have remained above T_c for longer than ~10 Ma. The thermal modeling shown in Fig. 6 reveals that this might be the case, at least for Estacado. All chronological data for Estacado plot on the "40 km" cooling curve but at that depth, cooling from peak temperatures might have started as late as ~20–30 Ma, significantly later than the Hf–W age of ~10 Ma. Therefore, in Estacado the Hf–W system might have closed before cooling started. Note, however, that both peak temperature and Hf–W closure temperature are not known precisely enough to clearly distinguish between these two endmember interpretations. Owing to the similarity of peak metamorphic and Hf–W closure temperature, both processes (i.e., cooling and increase in T_c due to grain coarsening) were probably important for H6 chondrites. In any case, the Hf–W age for H6 chondrites corresponds closely to the time of the thermal peak.

The Hf–W results appear to be most consistent with some of the models for the H chondrite parent body presented by Ghosh et al. (2003). In their models 3 and 4, accretion of the H chondrite parent body started at ~2 Ma and ended ~2–3.5 Ma later. Peak metamorphic temperatures in the centre are reached at ~5–6 Ma and although Ghosh et al. (2003) do not provide information on how long peak temperatures are maintained in their models 3 and 4, other thermal models indicate that in a body with ~100 km radius temperatures can be as high as ~900 °C at ~10 Ma (Miyamoto et al., 1981; Bouvier et al., 2007) (see also Fig. 6). Amelin et al. (2005) also found that the Pb–Pb dating results for Richardton are most consistent with the model 3 of Ghosh et al. (2003).

4.5. Hf–W fractionation among chondrite parent materials in the solar nebula

The initial ε^{182}W and initial ^{182}Hf/^{180}Hf obtained from the H chondrite isochrons can be used to constrain the time-integrated W isotope evolution, and hence ^{180}Hf/^{184}W ratio, of the H chondrite asteroid in comparison to average carbonaceous chondrites. The W isotope evolution of carbonaceous chondrites is given by the initial ε^{182}W and ^{182}Hf/^{180}Hf determined from internal CAI isochrons [ε^{182}W=−3.30±0.12; ^{182}Hf/^{180}Hf=(1.003±0.045)×10^{-4} (Burkhardt et al., submitted for publication)] and the precisely defined present-day ε^{182}W=−1.9±0.1 (Kleine et al., 2002; Schoenberg et al., 2002; Yin et al., 2002; Kleine et al., 2004a). These data indicate that carbonaceous chondrites evolved with ^{180}Hf/^{184}W=1.21, in excellent agreement with ^{180}Hf/^{184}W=1.210±0.075 (2σ) measured for 14 carbonaceous chondrites by isotope dilution (Kleine et al., 2004a). In the W isotope evolution diagram (Fig. 8), the analyzed H chondrites define a trend that is different from the evolution path of the carbonaceous chondrites, indicating that the H chondrite asteroid has ^{180}Hf/^{184}W=0.63±0.20. With this low ^{180}Hf/^{184}W the radiogenic ingrowth in H chondrite whole-rocks is small (~0.35 ε^{182}W in the first ~10 Ma), consistent with the very limited range in ε^{182}W of the H chondrite metals.

Compositional variations among the chondrite groups are commonly attributed to different proportions of several distinct components present in chondritic meteorites (Palme, 2001). Among these, CAIs [^{180}Hf/^{184}W~1.7, (Burkhardt et al., submitted for publication)] and metallic Fe (^{180}Hf/^{184}W~0) have Hf/W ratios different from those of average carbonaceous chondrites, such that different mixing proportions of CAIs and metal potentially can cause variations in Hf/W ratios among chondrite groups. Fig. 8 shows that the different Hf/W ratios must have been established in the first ~2 Ma of the solar system. Once more high-precision Hf–W isochrons for other chondrites (in particular LL chondrites with their probably high Hf/W ratios) are available, it should be possible to date the chemical fractionation among chondrites more precisely.

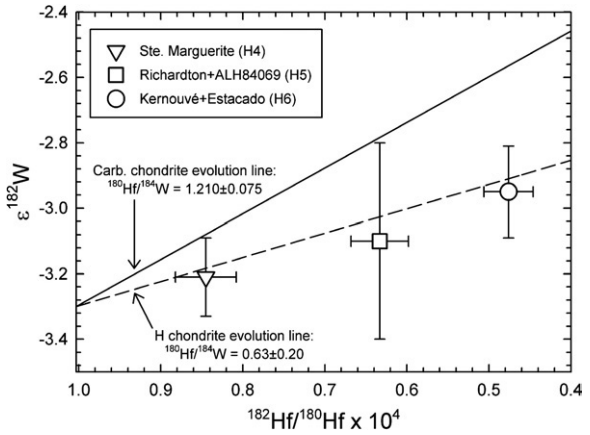

Fig. 8. W isotope evolution diagram for H chondrites. The carbonaceous chondrite evolution line is defined by their present-day ε^{182}W and the initial ε^{182}W of Allende CAIs. The analyzed H chondrites depart from the evolution line of carbonaceous chondrites, indicating evolution in a reservoir with a Hf/W ratio lower than that of carbonaceous chondrites.

5. Conclusions

Key issues regarding the accretion and early evolution of chondrite parent bodies include the timescales of chondrule formation and peak metamorphism. The relatively high closure temperature of the Hf–W system in high-Ca pyroxene makes internal Hf–W isochrons involving high-Ca pyroxene a powerful tool for obtaining such age constraints. Although it is more or less well established that most chondrules formed ~2–3 Ma later than CAIs (Russell et al., 1996; Kita et al., 2000; Kunihiro et al., 2004; Rudraswami and Goswami, 2007), this information is mainly based on Al–Mg ages for chondrules from only a few primitive chondrites. Most chondrites, however, are metamorphosed to some degree and even mild parent body metamorphism might reset the Al–Mg system. For instance, Kita et al. (2000) showed that Al–Mg ages for chondrules from chondrites of petrologic types higher than 3.4 are already partially reset. In contrast, Hf–W ages are more robust and less easily affected by thermal metamorphism and even for chondrites of petrologic type 4 appear to date chondrule formation. The capability of Hf–W chronometry for dating chondrule formation, however, will need to be assessed with more Hf–W ages for type 4 chondrites, by investigating the Hf–W systematics of type 3 chondrites and those ordinary chondrite groups for which Al–Mg chondrule ages are available.

The closure temperature of the Hf–W system in type 5 and 6 chondrites is essentially identical to their peak metamorphic temperatures, such that Hf–W ages for type 5 and 6 chondrites correspond closely to the time of the thermal peak. As we have shown here for the H chondrite parent body, such information is essential for constraining models for the thermal evolution of meteorite parent bodies, which is directly related to their accretion rate and terminal size. Formation intervals determined by Hf–W chronometry are much shorter than those obtained from Pb–Pb or Rb–Sr chronology because the Hf–W system closed early and hence preserved a record of the

earliest (i.e., high-temperature) evolution of chondrite parent bodies. Therefore, unlike other chronometers that have been used so far to constrain the (low-temperature) cooling history of chondrite parent bodies – such as the Pb–Pb, Rb–Sr and Ar–Ar systems – the Hf–W system is less easily disturbed by later events and hence appears most suitable for determining the initial thermal structure and metamorphic history of chondrite parent bodies. Hafnium–tungsten ages for chondrites should therefore permit the determination and direct comparison of accretion rate, terminal size, and thermal structure of chondrite parent bodies.

Acknowledgements

We thank Rainer Wieler for the comments and discussion. Conel Alexander and Jeff Grossmann are thanked for providing insights into chondrule mineralogy, especially regarding occurrence and grain sizes of high-Ca pyroxenes. Yuri Amelin is thanked for providing preprints of his unpublished work. We thank the Museum National d' Historie Naturelle (Paris), The National Museum of Natural History (Washington DC), The Natural History Museum (London), the Senckenbergmuseum (Frankfurt), and NASA for generously providing the samples for this study. Comments and suggestion from an anonymous reviewer and Mario Trieloff significantly improved the manuscript. Mario Trieloff pointed out the possibility that the ages for H6 chondrite may reflect early closure due to grain coarsening. We thank Rick Carlson for his comments and the efficient editorial handling of our manuscript. This study was supported by a Marie Curie post-doctoral fellowship to Thorsten Kleine.

References

Akridge, G., Benoit, P.H., Sears, D.W.G., 1998. Regolith and megaregolith formation of H-chondrites: thermal constraints on the parent body. Icarus 132, 185–195.
Alexander, C.M.D., 1994. Trace element microdistribution within ordinary chondrite chondrules: implications for chondrule formation conditions and precursors. Geochim. Cosmochim. Acta 58, 3451–3467.
Alexander, C.M.D., 2005. From supernovae to planets: the view from meteorites and interplanetary dust particles. In: Krot, A.N., Scott, E.R.D., Reipurth, B. (Eds.), Chondrites and the Protoplanetary Disk, Astronomical Society of the Pacific Conference Series 341.
Amelin, Y., 2008. U–Pb ages of angrites. Geochim. Cosmochim. Acta 72, 221–232.
Amelin, Y., Irving, A.J., 2007. Seven million years of evolution on the angrite parent body from Pb-isotopic data, Workshop on the chronology of meteorites and the early solar system, LPI Contribution No. 1374, pp. 1320–1321.
Amelin, Y., Ghosh, A., Rotenberg, E., 2005. Unraveling the evolution of chondrite parent asteroids by precise U–Pb dating and thermal modeling. Geochim. Cosmochim. Acta 69, 505–518.
Azough, F., Freer, R., 2000. Iron diffusion in single-crystal diopside. Phys. Chem. Miner. 27, 732–740.
Baker, J.A., Bizzarro, M., Wittig, N., Connelly, J., Haack, H., 2005. Early planetesimal melting from an age of 4.5662 Gyr for differentiated meteorites. Nature 436, 1127–1131.
Bennett, M.E., McSween, H.Y., 1996. Revised model calculations for the thermal histories of ordinary chondrite parent bodies. Meteorit. Planet. Sci. 31, 783–792.
Blinova, A., Amelin, Y., Samson, C., 2007. Constraints on the cooling history of the H-chondrite parent body from phosphate and chondrule Pb-isotopic dates from Estacado. Meteorit. Planet. Sci. 42, 1337–1350.
Bouvier, A., Blichert-Toft, J., Moynier, F., Vervoort, J.D., Albarède, F., 2007. Pb–Pb dating constraints on the accretion and cooling history of chondrites. Geochim. Cosmochim. Acta 71, 1583–1604.
Burkhardt, C., Kleine, T., Palme, H., Bourdon, B., Zipfel, J., Friedrich, J., Ebel, D., submitted for publication. Hf–W isochrons for CAIs and timescales for planetesimal accretion Geochim. Cosmochim. Acta.
Carslaw, H.S., Jaeger, J.C., 1959. Conduction of heat in solids. Oxford University Press.
Cherniak, D.J., 1998. Pb diffusion in clinopyroxene. Chem. Geol. 150, 105–117.
Cherniak, D.J., Lanford, W., Ryerson, F.J., 1991. Lead diffusion in apatite and zircon using ion implantation and Rutherford backscattering techniques. Geochim. Cosmochim. Acta 55, 1663–1673.
Clayton, R.N., Mayeda, T.K., 1996. Oxygen isotope studies of achondrites. Geochim. Cosmochim. Acta 60, 1999–2017.
Connelly, J., Amelin, Y., Bizzarro, M., Thrane, K., Baker, J.A., 2008. The Pb–Pb age of angrite Sah99555 revisited. Lunar Planet. Sci. Conf. XXXIX, 2386.pdf.
Cuzzi, J.N., Ciesla, F.J., Petaev, M.I., Krot, A.N., Scott, E.R.D., Weidenschilling, S.J., 2005. Nebular evolution of thermally processed solids: reconciling models and meteorites. In: Krot, A.N., Scott, E.R.D., Reipurth, B. (Eds.), Chondrites and the Protoplanetary Disk, Astronomical Society of the Pacific Conference Series 341, pp. 732–773.
Dodd, R.T., 1969. Metamorphism of the ordinary chondrites: a review. Geochim. Cosmochim. Acta 33, 161–203.
Dodd, R.T., 1981. Meteorites: A petrologic-chemical synthesis. Cambridge University Press, New York. 368 pp.
Dodson, M.H., 1973. Closure temperature in cooling geochronological and petrological systems. Contrib. Mineral. Petrol. 40, 259–274.
Ganguly, J., Tirone, M., 2001. Relationship between cooling rate and cooling age of a mineral: theory and applications to meteorites. Meteorit. Planet. Sci. 36, 167–175.
Ghosh, A., Weidenschilling, S.J., McSween, H.Y., 2003. Importance of the accretion process in asteroid thermal evolution: 6 Hebe as an example. Meteorit. Planet. Sci. 38, 711–724.
Göpel, C., Manhès, G., Allègre, C.J., 1994. U–Pb systematics of phosphates from equilibrated ordinary chondrites. Earth Planet. Sci. Lett. 121, 153–171.
Halliday, A.N., 2004. Mixing, volatile loss and compositional change during impact-driven accretion of the Earth. Nature 427, 505–509.
Harper, C.L., Jacobsen, S.B., 1996. Evidence for Hf-182 in the early solar system and constraints on the timescale of terrestrial accretion and core formation. Geochim. Cosmochim. Acta 60, 1131–1153.
Humayun, M., Campbell, A.J., 2002. The duration of ordinary chondrite metamorphism inferred from tungsten microdistribution in metal. Earth Planet. Sci. Lett. 198, 225–243.
Huss, G.R., Rubin, A.E., Grossman, J.N., 2006. Thermal metamorphism in chondrites. In: Lauretta, D.S., McSween, H.Y. (Eds.), Meteorites and the Early Solar System II. The University of Arizona Press, Tucson, pp. 567–586.
Jacobsen, S.B., 2005. The Hf–W isotopic system and the origin of the Earth and Moon. Ann. Rev. Earth Planet. Sci. 33, 531–570.
Kessel, R., Beckett, J.R., Stolper, E.M., 2007. The thermal history of equilibrated ordinary chondrites and the relationship between textural maturity and temperature. Geochim. Cosmochim. Acta 71, 1855–1881.
Kita, N.T., Nagahara, H., Togashi, S., Morishita, Y., 2000. A short duration of chondrule formation in the solar nebula: evidence from ^{26}Al in Semarkona ferromagnesian chondrules. Geochim. Cosmochim. Acta 64, 3913–3922.
Kleine, T., Münker, C., Mezger, K., Palme, H., 2002. Rapid accretion and early core formation on asteroids and the terrestrial planets from Hf–W chronometry. Nature 418, 952–955.
Kleine, T., Mezger, K., Münker, C., Palme, H., Bischoff, A., 2004a. ^{182}Hf–^{182}W isotope systematics of chondrites, eucrites, and Martian meteorites: chronology of core formation and mantle differentiation in Vesta and Mars. Geochim. Cosmochim. Acta 68, 2935–2946.
Kleine, T., Mezger, K., Palme, H., Scherer, E., Münker, C., 2004b. The W isotope evolution of the bulk silicate Earth: constraints on the timing and mechanisms of core formation and accretion. Earth Planet. Sci. Lett. 228, 109–123.
Kleine, T., Mezger, K., Palme, H., Scherer, E., Münker, C., 2005a. Early core formation in asteroids and late accretion of chondrite parent bodies: evidence from ^{182}Hf–^{182}W in CAIs, metal-rich chondrites and iron meteorites. Geochim. Cosmochim. Acta 69, 5805–5818.
Kleine, T., Mezger, K., Palme, H., Scherer, E., Münker, C., 2005b. The W isotope composition of eucrites metal: constraints on the timing and cause of the thermal metamorphism of basaltic eucrites. Earth Planet. Sci. Lett. 231, 41–52.
Kleine, T., Touboul, M., Halliday, A., Zipfel, J., Palme, H., 2007. Cosmochemical fractionation of Hf and W in the solar nebula: evidence from W isotopes in chondrites. Lunar Planet. Sci. XXXVIII.
Kleine, T., Bourdon, B., Burkhardt, C., Irving, A.J., 2008. Hf–W chronometry of angrites: constraints on the absolute age of CAIs and planetesimals accretion timescales. Lunar Planet. Sci. Conf. XXXIX, 2367.pdf.
Kong, P., Ebihara, M., 1996. Distribution of W and Mo in ordinary chondrites and implications for nebular and parent body thermal processes. Earth Planet. Sci. Lett. 137, 83–93.
Kunihiro, T., Rubin, A.E., McKeegan, K.D., Wasson, J.T., 2004. Initial ^{26}Al/^{27}Al in carbonaceous-chondrite chondrules: too little ^{26}Al to melt asteroids. Geochim. Cosmochim. Acta 68, 2947–2957.
Lindsley, D.H., 1983. Pyroxene thermometry. Am. Mineral. 68, 477–493.
Ludwig, K., 1991. ISOPLOT: a plotting and regression program for radiogenic isotope data; version 2.53, U.S.G.S. Open File Report 91-0445.
Lugmair, G.W., Galer, S.J.G., 1992. Age and isotopic relationships among the angrites Lewis Cliff 86010 and Angra dos Reis. Geochim. Cosmochim. Acta 56, 1673–1694.
Markowski, A., Quitté, G., Kleine, T., Halliday, A., Bizzarro, M., Irving, A.J., 2007. Hf–W chronometry of angrites and the earliest evolution of planetary bodies. Earth Planet. Sci. Lett. 262, 214–229.
Merk, R., Breuer, D., Spohn, T., 2002. Numerical modeling of 26Al-induced radioactive melting of asteroids considering accretion. Icarus 159, 183–191.
Min, K.W., Farley, K.A., Renne, P.R., Marti, K., 2003. Single grain (U–Th)/He ages from phosphates in Acapulco meteorite and implications for thermal history. Earth Planet. Sci. Lett. 209, 323–336.
Miyamoto, M., Fujii, N., Takeda, H., 1981. Ordinary chondrite parent body: an internal heating model. Proc. Lunar Planet. Sci. Conf. 12B, 1145–1152.
Münker, C., Weyer, S., Scherer, E., Mezger, K., 2001. Separation of high field strength elements (Nb, Ta, Zr, Hf) and Lu from rock samples for MC-ICPMS measurements. Geochem. Geophys. Geosyst. 2.
Nimmo, F., Agnor, C.B., 2006. Isotopic outcomes of N-body accretion simulations: constraints on equilibration processes during large impacts from Hf/W observations. Earth Planet. Sci. Lett. 243, 26–43.
Nimmo, F., Kleine, T., 2007. How rapidly did Mars accrete? Uncertainties in the Hf–W timing of core formation. Icarus 191, 497–504.
Palme, H., 2001. Chemical and isotopic heterogeneity in protosolar matter. Philos. Trans. R. Soc. London, A 359, 2061–2075.

Palme, H., Schultz, L., Spettel, B., Weber, H.W., Wänke, H., 1981. The Acapulco meteorite: chemistry, mineralogy and irradiation effects. Geochim. Cosmochim. Acta 45, 727–752.

Podosek, F.A., Brannon, J.C., 1991. Chondrite chronology by initial $^{87}Sr/^{86}Sr$ in phosphates? Meteoritics 26, 145–152.

Rambaldi, E.R., 1976. Trace element of metals from L-group chondrites. Earth Planet. Sci. Lett. 31, 224–238.

Righter, K., Shearer, C.K., 2003. Magmatic fractionation of Hf and W: constraints on the timing of core formation and differentiation in the Moon and Mars. Geochim. Cosmochim. Acta 67, 2497–2507.

Rudraswami, N.G., Goswami, J.N., 2007. Al-26 in chondrules from unequilibrated L chondrites: onset and duration of chondrule formation in the early solar system. Earth Planet. Sci. Lett. 257, 231–244.

Russell, S.S., Srinivasan, G., Huss, G.R., Wasserburg, G.J., Macpherson, G.J., 1996. Evidence for widespread ^{26}Al in the solar nebula and constraints on nebula time scales. Science 273, 757–762.

Salters, V.J.M., Hart, S.R., 1991. The mantle sources of ocean ridges, islands and arcs – the Hf-isotope connection. Earth Planet. Sci. Lett. 104, 364–380.

Schoenberg, R., Kamber, B.S., Collerson, K.D., Eugster, O., 2002. New W-isotope evidence for rapid terrestrial accretion and very early core formation. Geochim. Cosmochim. Acta 66, 3151–3160.

Scott, E.R.D., 2006. Meteoritical and dynamical constraints on the growth mechanisms and formation times of asteroids and Jupiter. Icarus 185, 72–82.

Shannon, R.D., 1976. Revised effective ionic radii and systematic studies of interatomic distances in halides and chalcogenides. Act. Crystall. A32, 751–767.

Slater-Reynolds, V., McSween, H.Y., 2005. Peak metamorphic temperatures in type 6 ordinary chondrites: an evaluation of pyroxene and plagioclase geothermometry. Meteorit. Planet. Sci. 40, 745–754.

Taylor, G.J., Maggiore, P., Scott, E.R.D., Rubin, A.E., Keil, K., 1987. Original structures, and fragmentation and reassembly histories of asteroids: evidence from meteorites. Icarus 69, 1–13.

Trieloff, M., Jessberger, E.K., Fieni, C., 2001. Comment on "Ar-40/Ar-39 age of plagioclase from Acapulco meteorite and the problem of systematic errors in cosmochronology" by Paul R. Renne. Earth Planet. Sci. Lett. 190, 267–269.

Trieloff, M., Jessberger, E.K., Herrwerth, I., Hopp, J., Fiéni, C., Ghelis, M., Bourot-Denise, M., Pellas, P., 2003. Structure and thermal history of the H-chondrite parent asteroid revealed by thermochronometry. Nature 422, 502–506.

Van Orman, J.A., Grove, T.L., Shimizu, N., 2001. Rare earth element diffusion in diopside: influence of temperature, pressure and ionic radius, and an elastic model for diffusion in silicates. Contrib. Mineral. Petrol. 141, 687–703.

Van Orman, J.A., Saal, A.E., Bourdon, B., Hauri, E.H., 2006. Diffusive fractionation of U-series radionuclides during mantle melting and shallow level melt-cumulate interaction. Geochim. Cosmochim. Acta 70, 4797–4812.

Walter, M.J., Thibault, Y., 1995. Partitioning of tungsten and molybdenum between metallic liquid and silicate melt. Science 270, 1186–1189.

Wasserburg, G.J., Papanastassiou, D.A., Sanz, H.G., 1969. Initial strontium for a chondrite and the determination of a metamorphism or formation interval. Earth Planet. Sci. Lett. 7, 33–43.

Watson, H.C., Watson, E.B., 2003. Siderophile trace element diffusion in Fe–Ni alloys. Phys. Earth Planet. Inter. 139, 65–75.

Weyer, S., Münker, C., Rehkamper, M., Mezger, K., 2002. Determination of ultra-low Nb, Ta. Zr and Hf concentrations and the chondritic Zr/Hf and Nb/Ta ratios by isotope dilution analyses with multiple collector ICP-MS. Chem. Geol. 187, 295–313.

Wlotzka, F., 2005. Cr spinel and chromite as petrogenetic indicators in ordinary chondrites: equilibration temperatures of petrologic types 3.7 to 6. Met. Planet. Sci. 40, 1673–1702.

Yin, Q.Z., Jacobsen, S.B., Yamashita, K., Blichert-Toft, J., Télouk, P., Albarède, F., 2002. A short timescale for terrestrial planet formation from Hf–W chronometry of meteorites. Nature 418, 949–952.